Midrapidity Antiproton-to-Proton Ratio from Au + Au Collisions at $\sqrt{s_{NN}} = 130$ GeV

C. Adler,[11] Z. Ahammed,[25] C. Allgower,[12] M. Anderson,[5] G. S. Averichev,[9] J. Balewski,[12] O. Barannikova,[9,25] L. S. Barnby,[15] J. Baudot,[13] S. Bekele,[22] V. V. Belaga,[9] R. Bellwied,[32] J. Berger,[11] H. Bichsel,[31] L. C. Bland,[12] C. O. Blyth,[3] B. E. Bonner,[26] R. Bossingham,[16] A. Boucham,[28] A. Brandin,[20] H. Caines,[22] M. Calderón de la Barca Sánchez,[33] A. Cardenas,[25] J. Carroll,[16] J. Castillo,[28] M. Castro,[32] D. Cebra,[5] S. Chattopadhyay,[32] M. L. Chen,[2] Y. Chen,[6] S. P. Chernenko,[9] M. Cherney,[8] A. Chikanian,[33] B. Choi,[29] W. Christie,[2] J. P. Coffin,[13] L. Conin,[28] T. M. Cormier,[32] J. G. Cramer,[31] H. J. Crawford,[4] M. DeMello,[26] W. S. Deng,[15] A. A. Derevschikov,[24] L. Didenko,[2] J. E. Draper,[5] V. B. Dunin,[9] J. C. Dunlop,[33] V. Eckardt,[18] L. G. Efimov,[9] V. Emelianov,[20] J. Engelage,[4] G. Eppley,[26] B. Erazmus,[28] P. Fachini,[27] M. I. Ferguson,[6] E. Finch,[33] Y. Fisyak,[2] D. Flierl,[11] K. J. Foley,[2] N. Gagunashvili,[9] J. Gans,[33] M. Germain,[13] F. Geurts,[26] V. Ghazikhanian,[6] J. Grabski,[30] O. Grachov,[32] D. Greiner,[16] V. Grigoriev,[20] E. Gushin,[20] T. J. Hallman,[2] D. Hardtke,[16] J. W. Harris,[33] M. Heffner,[5] S. Heppelmann,[23] T. Herston,[25] B. Hippolyte,[13] A. Hirsch,[25] E. Hjort,[25] G. W. Hoffmann,[29] M. Horsley,[33] H. Z. Huang,[6] T. J. Humanic,[22] H. Hümmler,[18] G. J. Igo,[6] A. Ishihara,[29] Yu. I. Ivanshin,[10] P. Jacobs,[16] W. W. Jacobs,[12] M. Janik,[30] I. Johnson,[16] P. G. Jones,[3] E. Judd,[4] M. Kaneta,[16] M. Kaplan,[7] D. Keane,[15] A. Khodinov,[20] A. Kisiel,[30] J. Klay,[5] S. R. Klein,[16] A. Klyachko,[12] A. S. Konstantinov,[24] L. Kotchenda,[20] A. D. Kovalenko,[9] M. Kramer,[21] P. Kravtsov,[20] K. Krueger,[1] C. Kuhn,[13] A. I. Kulikov,[9] G. J. Kunde,[33] C. L. Kunz,[7] R. Kh. Kutuev,[10] A. A. Kuznetsov,[9] J. Lamas-Valverde,[26] M. A. C. Lamont,[3] J. M. Landgraf,[2] S. Lange,[11] C. P. Lansdell,[29] B. Lasiuk,[33] F. Laue,[22] A. Lebedev,[2] T. LeCompte,[1] V. M. Leontiev,[24] P. Leszczynski,[30] M. J. LeVine,[2] Q. Li,[32] Q. Li,[16] S. J. Lindenbaum,[21] M. A. Lisa,[22] T. Ljubicic,[2] W. J. Llope,[26] G. LoCurto,[18] H. Long,[6] R. S. Longacre,[2] M. Lopez-Noriega,[22] W. A. Love,[2] D. Lynn,[2] L. Madansky,[14,*] R. Majka,[33] A. Maliszewski,[30] S. Margetis,[15] L. Martin,[28] J. Marx,[16] H. S. Matis,[16] Yu. A. Matulenko,[24] T. S. McShane,[8] Yu. Melnick,[24] A. Meschanin,[24] Z. Milosevich,[7] N. G. Minaev,[24] J. Mitchell,[14] V. A. Moiseenko,[10] D. Moltz,[16] C. F. Moore,[29] V. Morozov,[16] M. M. de Moura,[27] M. G. Munhoz,[27] G. S. Mutchler,[26] J. M. Nelson,[3] P. Nevski,[2] V. A. Nikitin,[10] L. V. Nogach,[24] B. Norman,[15] S. B. Nurushev,[24] J. Nystrand,[16] G. Odyniec,[16] A. Ogawa,[23] C. A. Ogilvie,[17] M. Oldenburg,[18] D. Olson,[16] G. Paic,[22] S. U. Pandey,[32] Y. Panebratsev,[9] S. Y. Panitkin,[15] A. I. Pavlinov,[32] T. Pawlak,[30] V. Perevoztchikov,[2] W. Peryt,[30] V. A. Petrov,[10] W. Pinganaud,[28] E. Platner,[26] J. Pluta,[30] N. Porile,[25] J. Porter,[2] A. M. Poskanzer,[16] E. Potrebenikova,[9] D. Prindle,[31] C. Pruneau,[32] S. Radomski,[30] G. Rai,[16] O. Ravel,[28] R. L. Ray,[29] S. V. RazinD. Reichhold,[8] J. Reid,[31] F. Retiere,[16] A. Ridiger,[20] H. G. Ritter,[16] J. B. Roberts,[26] O. V. Rogachevski,[9] C. Roy,[28] D. Russ,[7] V. Rykov,[32] I. Sakrejda,[16] J. Sandweiss,[33] A. C. Saulys,[2] I. Savin,[10] J. Schambach,[29] R. P. Scharenberg,[25] N. Schmitz,[18] L. S. Schroeder,[16] A. Schüttauf,[18] J. Seger,[8] D. Seliverstov,[20] P. Seyboth,[18] K. E. Shestermanov,[24] S. S. Shimanskii,[9] V. S. Shvetcov,[10] G. Skoro,[9] N. Smirnov,[33] R. Snellings,[16] J. Sowinski,[12] H. M. Spinka,[1] B. Srivastava,[25] E. J. Stephenson,[12] R. Stock,[11] A. Stolpovsky,[32] M. Strikhanov,[20] B. Stringfellow,[25] H. Stroebele,[11] C. Struck,[11] A. A. P. Suaide,[2,7] E. Sugarbaker,[22] C. Suire,[13] T. J. M. Symons,[1,6] A. Szanto de Toledo,[27] P. Szarwas,[30] J. Takahashi,[27] A. H. Tang,[15] J. H. Thomas,[16] V. Tikhomirov,[20] T. Trainor,[31] S. Trentalange,[6] M. Tokarev,[9] M. B. Tonjes,[19] V. Trofimov,[20] O. Tsai,[6] K. Turner,[2] T. Ullrich,[33] D. G. Underwood,[1] G. Van Buren,[2] A. M. VanderMolen,[19] A. Vanyashin,[16] I. M. Vasilevski,[10] A. N. Vasiliev,[24] S. E. Vigdor,[12] S. A. Voloshin,[32] F. Wang,[25] H. Ward,[29] R. Wells,[22] T. Wenaus,[2] G. D. Westfall,[19] C. Whitten, Jr.,[6] H. Wieman,[16] R. Willson,[22] S. W. Wissink,[12] R. Witt,[15] N. Xu,[16] Z. Xu,[33] A. E. Yakutin,[24] E. Yamamoto,[6] J. Yang,[6] P. Yepes,[26] A. Yokosawa,[1] V. I. Yurevich,[9] Y. V. Zanevski,[9] J. Zhang,[16] W. M. Zhang,[15] R. Zoulkarneev,[10] and A. N. Zubarev[9]

[1]*Argonne National Laboratory, Argonne, Illinois 60439*
[2]*Brookhaven National Laboratory, Upton, New York 11973*
[3]*University of Birmingham, Birmingham, United Kingdom*
[4]*University of California, Berkeley, California 94720*
[5]*University of California, Davis, California 95616*
[6]*University of California, Los Angeles, California 90095*
[7]*Carnegie Mellon University, Pittsburgh, Pennsylvania 15213*
[8]*Creighton University, Omaha, Nebraska 68178*
[9]*Laboratory for High Energy (JINR), Dubna, Russia*
[10]*Particle Physics Laboratory (JINR), Dubna, Russia*
[11]*University of Frankfurt, Frankfurt, Germany*
[12]*Indiana University, Bloomington, Indiana 47408*
[13]*Institut de Recherches Subatomiques, Strasbourg, France*
[14]*The Johns Hopkins University, Baltimore, Maryland 21218*

 0031-9007/01/86(21)/4778(5)$15.00

[15]*Kent State University, Kent, Ohio 44242*
[16]*Lawrence Berkeley National Laboratory, Berkeley, California 94720*
[17]*Massachusetts Institute of Technology, Cambridge, Massachusetts 02139*
[18]*Max-Planck-Institut für Physik, Munich, Germany*
[19]*Michigan State University, East Lansing, Michigan 48824*
[20]*Moscow Engineering Physics Institute, Moscow, Russia*
[21]*City College of New York, New York City, New York 10031*
[22]*Ohio State University, Columbus, Ohio 43210*
[23]*Pennsylvania State University, University Park, Pennsylvania 16802*
[24]*Institute of High Energy Physics, Protvino, Russia*
[25]*Purdue University, West Lafayette, Indiana 47907*
[26]*Rice University, Houston, Texas 77251*
[27]*Universidade de Sao Paulo, Sao Paulo, Brazil*
[28]*SUBATECH, Nantes, France*
[29]*University of Texas, Austin, Texas 78712*
[30]*Warsaw University of Technology, Warsaw, Poland*
[31]*University of Washington, Seattle, Washington 98185*
[32]*Wayne State University, Detroit, Michigan 48201*
[33]*Yale University, New Haven, Connecticut 06520*
(Received 27 December 2000)

We report results on the ratio of midrapidity antiproton-to-proton yields in Au + Au collisions at $\sqrt{s_{NN}} = 130$ GeV per nucleon pair as measured by the STAR experiment at RHIC. Within the rapidity and transverse momentum range of $|y| < 0.5$ and $0.4 < p_t < 1.0$ GeV/c, the ratio is essentially independent of either transverse momentum or rapidity, with an average of $0.65 \pm 0.01_{(\mathrm{stat})} \pm 0.07_{(\mathrm{syst})}$ for minimum bias collisions. Within errors, no strong centrality dependence is observed. The results indicate that at this RHIC energy, although the p-$\overline{p}$ pair production becomes important at midrapidity, a significant excess of baryons over antibaryons is still present.

DOI: 10.1103/PhysRevLett.86.4778 PACS numbers: 25.75.Ld

Lattice quantum chromodynamics calculations predict that at sufficiently high energy density a phase transition from hadronic matter to a state of deconfined quarks and gluons [1,2] will occur. To create and study this deconfined state is the primary goal of the heavy-ion collision program at the Relativistic Heavy Ion Collider (RHIC) [1]. However, the formation of such a deconfined state depends on the initial conditions of the matter created at the early stage of heavy-ion collisions. Baryon number transport (or stopping), achieved mostly at the early stage, is one of the important observables [3,4] for high-energy collisions, since the degree of baryon stopping affects the overall dynamical evolution of these collisions. It affects the processes of initial parton equilibration [5–8], particle production [1], thermal and/or chemical equilibration [9], and the development of collective expansion [10,11]. Information on baryon transport may be experimentally accessed by the measurement of the ratio of the antiproton-to-proton yields ($\overline{p}/p$).

In this Letter, we report results on the inclusive $\overline{p}/p$ ratio in Au + Au collisions at the center of mass energy $\sqrt{s_{NN}} = 130$ GeV per nucleon pair measured by the solenoidal tracker at RHIC (STAR).

The STAR detector consists of several detector subsystems in a large solenoidal magnet. The STAR time projection chamber (TPC) [12] is 4.2 m long, with a 50 cm inner radius and a 2 m outer radius. For minimum ionizing particles in P-10 (90% argon, 10% methane) gas, approximately 45 primary electrons are produced per centimeter of track. This ionization was measured on 45 pad rows. The system could accommodate ionization from 200 MeV/c protons without saturation and its noise level was about 5% of minimum ionizing. More details of the detector can be found elsewhere [13,14]. For the data taken in the year 2000 run and presented here, the main setup consists of the TPC, a scintillator trigger barrel (CTB) surrounding the TPC, and two zero degree calorimeters [15] located upstream and downstream along the axis of the TPC and beams. The TPC was operated in a 0.25 T magnetic field. The CTB measures the total energy deposition in the scintillator from charged particles, and the ZDCs measure beamlike neutrons from fragmentation and/or evaporation of the colliding nuclei. The coincidence of the ZDCs and RHIC beam crossing was the experimental trigger for the minimum bias events used in this analysis.

The collision centrality was determined off line from the measured total charged particle multiplicity in the pseudorapidity range of $|\eta| < 0.75$. As was done in [11], the total charged multiplicity was scaled by the maximum value measured, and the distribution of the scaled multiplicity was subdivided into eight centrality bins.

For this analysis, 68×10^3 minimum bias events were used with an event vertex $|z| \leq 50$ cm. Protons and antiprotons were selected according to specific energy loss (dE/dx) in the TPC up to a momentum of 1 GeV/c. A mean dE/dx for each track was obtained by averaging the lower 70% of the measured dE/dx values. This

selection reduces our sensitivity to large fluctuations in the dE/dx measurements. At a momentum of 0.5 GeV/c, the dE/dx resolution was found to be 8% for a typical long track in the TPC. Figure 1 shows the midrapidity ($|y| < 0.1$) particle raw yields as a function of $Z = \ln[(dE/dx)_{\rm exp}/(dE/dx)_{\rm BB}]$, where $(dE/dx)_{\rm BB}$ is the expected dE/dx value. The proton mass was used in the Bethe-Bloch $(dE/dx)_{\rm BB}$ calculations so the Z distributions of proton (antiproton) are centered about zero in those plots. The dashed lines are the multi-Gaussian fits to the Z distributions (including pions, kaons, and protons). Protons and antiprotons with $p_t > 175$ MeV/c were reconstructed. Within the acceptance the typical momentum resolution was 2% and the systematic uncertainty in the proton (antiproton) yields, extracted from the dE/dx fitting, was less than 2%. Tracks were selected if their distance of closest approach to the primary vertex were less than 3 cm, and if they had at least 15 out of 45 possible TPC space points. Several tests showed that the $\overline{p}/p$ results were not sensitive to variations of these cuts within reasonable ranges. The raw yields of protons and antiprotons were obtained by fitting the Z distributions (see Fig. 1) for each given (y, p_t) bin, and were used to obtain the $\overline{p}/p$ ratio.

The STAR TPC is symmetric about midrapidity and has full azimuthal coverage. Because of this symmetry, most of the detector effects are the same for protons and antiprotons and cancel in the $\overline{p}/p$ ratio. However, there are two important differences which are mostly dominant at low momentum: (i) background protons are produced in the detector materials via hadronic interactions [16], and (ii) some of the antiprotons are absorbed in the detector materials.

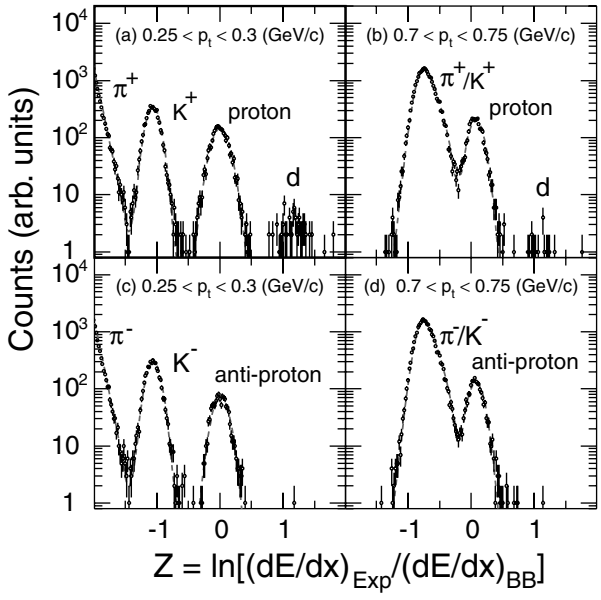

FIG. 1. Midrapidity particle yields as a function of $Z = \ln[(dE/dx)_{\rm exp}/(dE/dx)_{\rm BB}]$ from minimum bias Au + Au events. Top two plots (a) and (b) and bottom plots (c) and (d) are for positive particles and negative particles, respectively. Proton mass was used in the Bethe-Bloch $(dE/dx)_{\rm BB}$ calculations so the Z distributions of proton are centered about zero. Dashed lines are the multi-Gaussian fits to the measured distributions.

Background protons are evident from the distribution of the distance of closest approach (dca). The distribution is peaked at small dca and has a flat tail from secondary production which extends in to the peak region where primary tracks are centered. Since the background shape of the dca distribution at small dca ($\leq$3 cm) is not accessible from the data, a Monte Carlo (MC) simulation (GEANT [17]) was employed using as input particles generated by both HIJING [18] and RQMD [19] models. An empirical form was found for the background:

$$\text{background}(dca) \propto \left[1 + \exp\left(\frac{dca - dca_0}{a}\right)\right]^{-1}, \quad (1)$$

where the parameters dca_0 and a were obtained by fitting to the MC results. In general these parameters are momentum dependent and the normalization factor was obtained from the data. In the momentum region around 0.2 GeV/c, the number of background protons was found to be twice the number of primary protons. This leads to a rather large systematic uncertainty in the raw proton yield. Therefore, in this analysis we limited ourselves to the region where systematic errors are below 10% leading to a lower p_t cutoff at 0.4 GeV/c. At the high momentum end, $p \approx 1$ GeV/c, the dE/dx method becomes insufficient for particle identification.

The antiproton absorption loss was estimated via

$$\text{absorption} = 1 - \exp(-\sigma_{\rm anni}\rho_t p/p_t), \quad (2)$$

where ρ_t is the transverse area density of nucleons in the materials. p and p_t are the antiproton total momentum and transverse momentum, respectively. The annihilation cross section was parametrized as $\sigma_{\rm anni} = 1.2\sigma_{\rm tot}/\sqrt{s}$, where $\sqrt{s}$ is the center-of-mass energy of the p-$\overline{p}$ pair in GeV, and a power-law parametrization for the total p-$\overline{p}$ cross section $\sigma_{\rm tot}$ from Ref. [20] was used. For consistency, we also checked the above parametrization for antiproton absorption loss in the TPC with the results of a full MC simulation for the STAR TPC. The results are consistent and within the kinematic region of $0.4 < p_t < 1.0$ GeV/c, the $\overline{p}$ absorption loss was found to be less than 5%.

In this paper, we report the inclusive $\overline{p}/p$ ratios and no attempts have been made to correct for feed-down protons and antiprotons from hyperon weak decays. Such corrections would inevitably depend on the assumptions for hyperon and antihyperon yields and momentum distributions. However, if antihyperon to hyperon ratios are the same as the $\overline{p}/p$ ratio, then weak-decay feed-downs would not affect the $\overline{p}/p$ ratio. Using the HIJING [18] results as input, MC simulations show that about 81% of the Λ-decay protons were reconstructed with $dca < 3$ cm and 65% with $dca < 1$ cm. As expected, the fractions are the same for antiprotons. For a systematic check, some of the hyperon

feed-down effects were studied from the data by varying the dca cut. The results show that the $\overline{p}/p$ ratio decreases by about 2% from $dca = 3$ cm to 1 cm cut. These effects were not included in the systematic errors estimated below.

For this measurement, systematic errors mainly come from two sources: (i) The systematic uncertainty in proton background in relatively low transverse momentum region ($p_t < 0.4$ GeV/c). As mentioned above, the background protons were estimated via the detailed GEANT [17] simulation of the TPC. By varying the dca cut, the systematic error on the determination of number of protons is $\leq$10% at $p_t \sim 0.4$ GeV/c and drops to $<$2% at $p_t \sim 0.6$ GeV/c. (ii) As one will see in Fig. 2(b), there is an asymmetry between positive and negative rapidities. The asymmetry is less than 7%. The origin of the asymmetry is not fully understood and therefore it is included in the overall systematic errors for the $\overline{p}/p$ ratio. Other uncertainties like contamination in particle identification (most at high p_t) and the centrality dependence of the systematic errors are estimated much smaller, and are not included in the overall systematic errors.

Figure 2(a) shows the minimum bias $\overline{p}/p$ ratio as a function of p_t in the rapidity range of $0.3 < |y| < 0.4$. The ratio is 0.65 and is consistent with a constant value in the p_t range of $0.4 < p_t < 1.0$ GeV/c. The systematic error is estimated to be 10% for the lowest p_t bin, mainly due to proton background. At higher p_t the systematic error is less than 7%. Figure 2(b) shows the $\overline{p}/p$ ratio integrated over $0.6 < p_t < 0.8$ GeV/c as a function of rapidity. In this kinematic region, systematic errors are estimated to be less than 10%. Within errors, the ratio is consistent with a constant in the measured rapidity range.

Figure 2(c) shows the centrality dependence of $\overline{p}/p$ integrated over $|y| < 0.3$ and $0.6 < p_t < 0.8$ GeV/c. Although the ratio is consistent with a constant, there is an indication of a systematic drop from peripheral to central collisions. At lower bombarding energies, the value of the $\overline{p}/p$ ratio decreases by a factor of 2 with increasing centrality for Au + Au collisions at the Alternating Gradient Synchrotron (AGS) [21,22] and a factor of 1.6 for Pb + Pb collisions at the Super Proton Synchrotron (SPS) [23–27]. These low energy results are consistent with more baryon stopping and/or nucleon-$\overline{p}$ annihilation in central collisions relative to peripheral collisions. A similar picture may also apply to the RHIC results presented here.

At this RHIC energy, the $\overline{p}/p$ ratio is significantly smaller than unity over the measured centrality range, indicating an overall excess of protons over antiprotons in the midrapidity region. This implies that a certain fraction of the baryon number is transported from the incoming nucleus at beam rapidity to the midrapidity region even in peripheral Au + Au collisions at $\sqrt{s_{NN}} = 130$ GeV. Thus at this RHIC energy, the midrapidity region is not yet net-baryon free.

On the other hand, there is a dramatic increase in the midrapidity $\overline{p}/p$ ratio in central heavy-ion collisions in going from AGS ($\overline{p}/p = 0.000\,25 \pm 10\%$) [21] to SPS

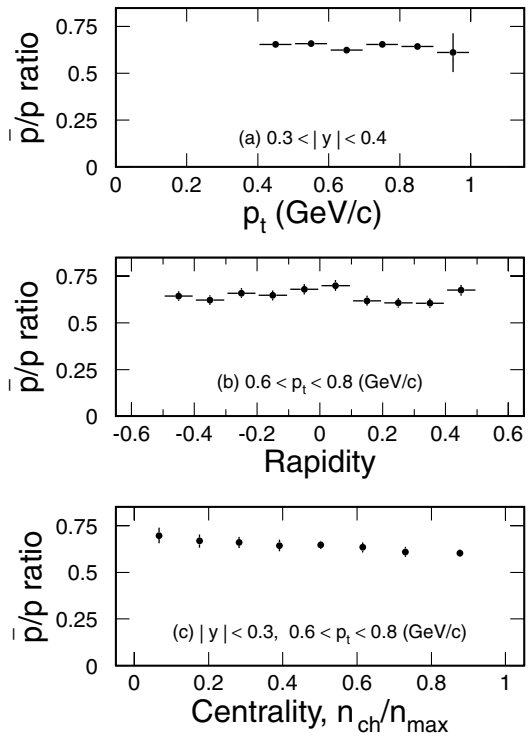

FIG. 2. The antiproton-to-proton ratios (a) as a function of transverse momentum p_t over the rapidity range $0.3 < |y| < 0.4$; (b) as a function of rapidity within $0.6 < p_t < 0.8$ GeV/c; and (c) as a function of the collision centrality within $|y| < 0.3$ and $0.6 < p_t < 0.8$ GeV/c. (a) and (b) are for minimum bias collisions. Errors are statistical only. The overall systematic errors are estimated to be 10%.

($\overline{p}/p \approx 0.07 \pm 10\%$) [25–27] and to RHIC. This is demonstrated in Fig. 3 where the central heavy-ion results are shown as a function of the center of mass energy $\sqrt{s_{NN}}$. For comparison, also shown in Fig. 3, are the $\overline{p}/p$ ratios in $p + p$ collisions at midrapidity and averaged over $0.35 < p_t < 0.6$ GeV/c [28]. The kinematic coverage for the $p + p$ collisions is similar to this measurement. The value of the $\overline{p}/p$ ratio from RHIC is close to or even larger than that in $p + p$ collisions at $\sqrt{s_{NN}} = 53$ GeV. Note that the beam rapidities at $\sqrt{s_{NN}} = 53$ and 130 GeV are 4.0 and 4.9, respectively.

For comparison, the HIJING(v1.35) model [18] predicts a $\overline{p}/p$ ratio of approximately 0.8 for Au + Au central collisions at $\sqrt{s_{NN}} = 130$ GeV. If the baryon junction mechanism [4] is considered, the ratio is 0.75. In contrast, the Relativistic Quantum Molecular Dynamics RQMD(v2.4) model [19] predicts a $\overline{p}/p$ ratio increasing with p_t with an average value of approximately 0.5. Note that the HIJING model is motivated by perturbative QCD but does not have late stage rescattering, and the RQMD model has late stage hadronic rescattering. As a result, the RQMD calculations predict a p_t dependence of the $\overline{p}/p$ ratio (from 0.2 to 0.55 in $p_t \leq 1$ GeV/c) while a constant ratio is observed from the HIJING calculations.

In summary, we have reported the ratio of the midrapidity antiproton to proton yields in Au + Au collisions

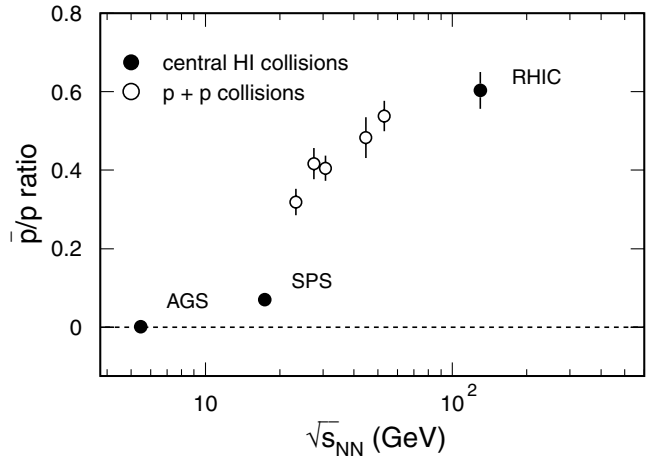

FIG. 3. Midrapidity antiproton-to-proton ratio ($\overline{p}/p$) measured in central heavy-ion collisions (filled symbols) and elementary $p + p$ collisions (open symbols). The left end of the abscissa is the p-$\overline{p}$ pair production threshold in $p + p$ ($\sqrt{s_{NN}} = 3.75$ GeV). The RHIC data is the most central point from Fig. 2c. Errors, either shown or smaller than the symbol size, are statistical and systematic errors added in quadrature.

at $\sqrt{s_{NN}} = 130$ GeV measured by the STAR experiment. Within the rapidity and transverse momentum range of $|y| < 0.5$ and $0.4 < p_t < 1.0$ GeV/c, the ratio is essentially independent of either transverse momentum or rapidity. In this kinematic range, the average $\overline{p}/p$ ratio is found to be $0.65 \pm 0.01_{(\mathrm{stat})} \pm 0.07_{(\mathrm{syst})}$ for minimum bias collisions. No strong centrality dependence is observed in the centrality range measured. The value of the $\overline{p}/p$ ratio indicates that although p-$\overline{p}$ pair production becomes important at midrapidity, a significant excess of baryons over antibaryons is still present in heavy-ion collisions at RHIC. Comparisons of our result to heavy-ion results at lower energies indicate that the midrapidity $\overline{p}/p$ ratio in heavy-ion collisions increases significantly with the collision energy.

We wish to thank the RHIC Operations Group at Brookhaven National Laboratory for their tremendous support and for providing collisions for the experiment. This work was supported by the Division of Nuclear Physics and the Division of High Energy Physics of the Office of Science of the U.S. Department of Energy, the United States National Science Foundation, the Bundesministerium für Bildung und Forschung of Germany, the Institut National de la Physique Nucleaire et de la Physique des Particules of France, the United Kingdom Engineering and Physical Sciences Research Council, and the Russian Ministry of Science and Technology.

*Deceased.

[1] For reviews and recent developments, see *Quark Matter '99 Proceedings* [Nucl. Phys. **A661** (1999)].
[2] F. Karsch, E. Laermann, and A. Peikert, Phys. Lett. B **478**, 447 (2000).
[3] W. Busza and A. S. Goldhaber, Phys. Lett. **B139**, 235 (1984).
[4] S. E. Vance, M. Gyulassy, and X. N. Wang, Phys. Lett. B **443**, 45 (1998); S. E. Vance, Nucl. Phys. **A661**, 230c (1999).
[5] X. N. Wang and M. Gyulassy, Phys. Rev. Lett. **68**, 1480 (1992).
[6] M. Gyulassy and X. N. Wang, Nucl. Phys. **B420**, 583 (1994).
[7] R. Baier, Yu. L. Dokshitzer, S. Peigne, and D. Schiff, Phys. Lett. B **345**, 277 (1995).
[8] X. N. Wang, Phys. Rev. D **43**, 104 (1991).
[9] P. Braun-Munzinger, I. Heppe, and J. Stachel, Phys. Lett. B **465**, 15 (1999).
[10] NA44 Collaboration, I. G. Bearden *et al.,* Phys. Rev. Lett. **78**, 2080 (1997).
[11] STAR Collaboration, K. H. Ackermann *et al.,* Phys. Rev. Lett. **86**, 402 (2001).
[12] H. Wieman *et al.,* IEEE Trans. Nucl. Sci. **44**, 671 (1997).
[13] W. Betts *et al.,* IEEE Trans. Nucl. Sci. **44**, 592 (1997); S. Klein *et al.,* IEEE Trans. Nucl. Sci. **43**, 1768 (1996).
[14] STAR Collaboration, K. H. Ackermann *et al.,* Nucl. Phys. **A661**, 681c (1999).
[15] C. Adler, A. Denisov, E. Garcia, M. Murray, H. Strobele, and S. White, LANL Report No. nucl-ex/0008005, 2000.
[16] D. Ashery and J. P. Schiffer, Annu. Rev. Nucl. Part. Sci. **36**, 207 (1986).
[17] P. Nevski, in Proceedings of the International Conference on Computing in High Energy and Nuclear Physics, Padova, Italy, 2000 (to be published).
[18] X. N. Wang, Phys. Rep. **280**, 287 (1997).
[19] H. Sorge, Phys. Rev. C **52**, 3291 (1995).
[20] Particle Data Group, Eur. Phys. J. C **3**, 207 (1998).
[21] E802 Collaboration, L. Ahle *et al.,* Phys. Rev. Lett. **81**, 2650 (1998).
[22] E814 Collaboration, J. Barrette *et al.,* Z. Phys. C **59**, 211 (1993).
[23] NA49 Collaboration, H. Appelshauser *et al.,* Phys. Rev. Lett. **82**, 2471 (1999).
[24] NA44 Collaboration, I. G. Bearden *et al.,* Phys. Lett. B **388**, 431 (1996).
[25] NA44 Collaboration, M. Kaneta *et al.,* J. Phys. G **23**, 1865 (1997).
[26] NA49 Collaboration, F. Siklér *et al.,* Nucl. Phys. **A661**, 45c (1999).
[27] G. E. Cooper, Ph.D. thesis, University of California at Berkeley, 2000.
[28] A. M. Rossi *et al.,* Nucl. Phys. **B84**, 269 (1975); M. Aguilar-Benitez *et al.,* Z. Phys. C **50**, 405 (1991).